Basic RF Characteristics of Fishbone-Type Transmission Line Employing Comb-Type Ground Plane (FTLCGP) on PES Substrate for Use in Flexible Passive Circuits

Young Yun, Jang-Hyeon Jeong, Hong Seung Kim, and Nakwon Jang

In this work, a fishbone-type transmission line employing a comb-type ground plane (FTLCGP) was fabricated on polyethersulfone (PES) substrate, and its RF characteristics were thoroughly investigated. According to the results, it was found that the FTLCGP on PES showed periodic capacitance values much higher than other types of transmission lines due to a coupling capacitance between the signal line and ground, which resulted in a reduction of wavelength and line width. Using the theoretical analysis, we also extracted the bandwidth characteristic of the FTLCGP on PES. According to the result, the FTLCGP structure showed a cut-off frequency of 280 GHz.

Keywords: Fishbone-type transmission line employing comb-type ground plane, FTLCGP, polyethersulfone, PES, Monolithic Microwave Integrated Circuit, MMIC.

Manuscript received Feb. 27, 2014; revised Mar. 21, 2014; accepted Apr. 1, 2014.

This research was financially supported by the Ministry of Education, Science Technology (MEST) and National Research Foundation of Korea (NRF) through the Human Resource Training Project for Regional Innovation. This work was supported by the National Research Foundation of Korea (NRF) grant funded by the Korea government (MSIP) (2014R1A2A1A11049844).

Young Yun (corresponding author, yunyoung@kmou.ac.kr) and Jang-Hyeon Jeong (jjh2010@ kmou.ac.kr) are with the Department of Radio Communication Engineering, Korea Maritime and Ocean University, Busan, Rep. of Korea.

Hong Seung Kim (hongseung@kmou.ac.kr) is with the Department of Nano Semiconductor Engineering, Korea Maritime and Ocean University, Busan, Rep. of Korea.

Nakwon Jang (nwjang@kmou.ac.kr) is with the Department of Electrical and Electronics Engineering, Korea Maritime and Ocean University, Busan, Rep. of Korea.

I. Introduction

Flexible electron devices have been employed for applications such as flexible displays, smart tags, and wearable products [1]. Recently, RF applications of flexible electron devices have drawn attention due to the demand for the development of foldable wireless communication devices. Compared with other flexible materials, polyethersulfone (PES) showed better heat-resisting properties and higher transparency [2]–[3]. In addition, PES shows good water-resistant qualities [2]. For these reasons, PES has been employed in flexible Monolithic Microwave Integrated Circuits (MMICs) [4]–[5]. The coefficient of thermal expansion and glass transition temperature of PES is 49.1 ppm/K and 228°C, respectively, and the dielectric loss tangent and relative permittivity of PES is 0.001 and 3.5, respectively. Silicon substrate is a widely used commercial semiconducting material. So, the electrical characteristics of many new materials are often compared to those of silicon. The electrical properties of PES were also compared with the silicon substrate. According to our previous results, [4]–[5], it was found that the insertion loss of PES was much lower than that of silicon substrate. To reduce the size of the RF device on semiconducting substrate, we should use a transmission line with a short wavelength. However, the wavelength of the transmission line on PES was much longer than that on conventional semiconducting substrate, such as silicon, due to its low effective permittivity [4]. Usually, a transmission line

with low impedance is required for the impedance matching of a transistor in high frequency due to the low input and output impedance of transistors. However, the transmission line on PES showed a characteristic impedance much higher than that shown on conventional semiconducting substrate.

For a PES substrate of thickness 200 μm, a coplanar waveguide having a line width of 50 μm and gap (a gap between line and ground) of 65 μm on the PES showed a characteristic impedance higher than 100 Ω. Therefore, a transmission line with a very wide line width is required to perform the impedance matching of transistors with low input and output impedance [4]. For this reason, the passive components on a PES substrate have to be a little larger in size than those on a conventional semiconducting substrate. To solve the above problem, the fishbone-type transmission line (FTTL) was proposed, and its RF characteristics were evaluated [4]. According to the results in [4], the FTTL on the PES showed an effective permittivity (ε_{eff}) that was much higher than that shown by a conventional coplanar waveguide on PES, and this resulted in a reduction in wavelength. In addition, the FTTL on the PES showed a lower characteristic impedance than that of the coplanar waveguide on PES due to an enhancement of the periodic capacitance.

Recently, we have proposed a fishbone-type transmission line employing a comb-type ground plane (FTLCGP) for a further reduction of the RF device on PES [5]. The size of the impedance transformer employing the FTLCGP was highly reduced compared with the conventional one [5]. For application to various on-chip components on flexible MMICs, the basic characteristics of the FTLCGP structure on PES should be thoroughly explored. However, an extensive investigation of the basic characteristics of the FTLCGP structure on PES has not yet been performed.

In this work, basic RF characteristics of FTLCGP on PES are theoretically studied using a simple equivalent circuit and closed-form equations. Concretely, RF characteristics such as impedance and bandwidth are extracted from the theoretical analysis, which offered a design guideline for passive components employing FTLCGP. According to our results, we found that the theoretical results showed good agreement with the experimental ones. The basic RF characteristics of the FTLCGP structure obtained from the experimental and theoretical analysis indicated that the FTLCGP structure can be effectively used for a development of RF components on flexible PES substrates.

II. FTLCGP Structure on PES

Figure 1 shows the structure of the FTTL [4] on PES. The conventional coplanar waveguide has only a periodical

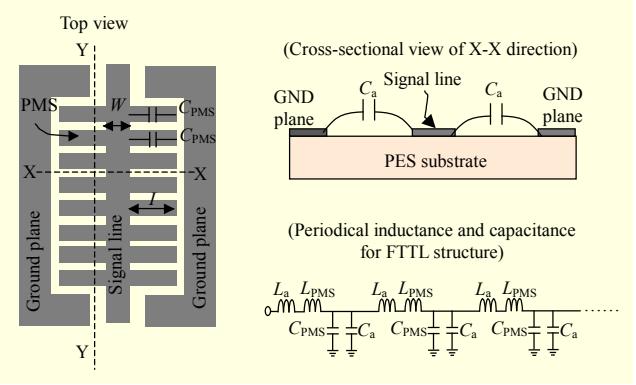

Fig. 1. Structure of FTTL on PES [4].

capacitance, C_a, between line and ground plane, while the FTTL has an additional periodical shunt capacitance, C_{PMS} [4]. In addition, the coplanar waveguide has only a periodical inductance, L_a, due to the current flowing across the signal line, while the FTTL has an additional inductance, L_{PMS}, due to the current flowing across the PMS. The FTTL on PES showed a much higher periodic capacitance and inductance than that of a conventional coplanar waveguide on PES, which led to a reduction of wavelength and characteristic impedance [4].

In this work, a modified structure, FTLCGP, was fabricated on PES for a further reduction of wavelength and characteristic impedance. The wavelength and characteristic impedance of a transmission line can respectively be expressed as follows [6]:

$$\lambda = \frac{2\pi}{\beta} \approx \frac{2\pi}{\omega\sqrt{LC}}, \tag{1}$$

$$Z_0 = \sqrt{\frac{L}{C}}, \tag{2}$$

where ω, L, and C are the angular frequency, periodic series inductance, and shunt capacitance of the transmission line, respectively. In particular, C is a periodic shunt capacitance due to a coupling between the signal line and ground. From the above equations, we can see that the periodic shunt capacitance between the signal line and ground should be increased to reduce wavelength and characteristic impedance. In the proposed FTLCGP, a periodic ground structure was employed to enhance the periodic shunt capacitance. Figure 2 shows the structure of the FTLCGP. As shown in this figure, the FTLCGP consists of a fishbone-type center line and comb-type ground planes. The fishbone-type center line consists of a signal line and periodic metal strips (PMSs), and the comb-type ground plane consists of a ground plane and periodic ground strips (PGSs). The PMSs are placed alternately with the PGSs. Therefore, compared with the FTTL, the FTLCGP has an additional shunt capacitance between the signal line and ground (C_b) due to an electromagnetic coupling between the

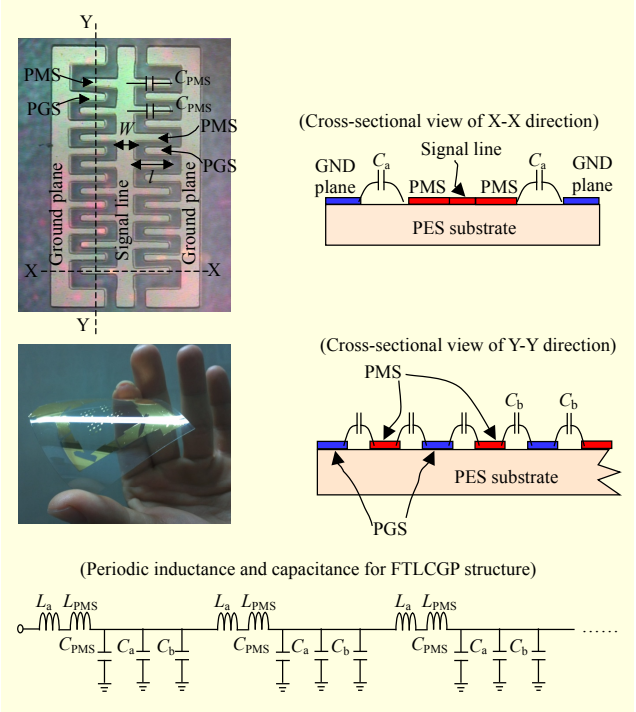

Fig. 2. Structure of FTLCGP on PES.

PMSs and PGSs, which increases the total periodic shunt capacitance. Therefore, the total periodic shunt capacitance of the FTTL and FTLCGP can be expressed as follows:

$$C_{\mathrm{FTTL}} = C_{\mathrm{a}} + C_{\mathrm{PMS}}, \tag{3}$$

$$C_{\mathrm{FTLCGP}} = C_{\mathrm{a}} + C_{\mathrm{PMS}} + C_{\mathrm{b}}. \tag{4}$$

In the FTTL structure, there is a coupling capacitance between the PMSs. However, to contribute to a reduction in wavelength, the coupling capacitance should exist between the signal line and ground, because the C in (1) and (2) is the shunt capacitance between the signal line and ground. From (1) and (2), we can obtain the following equation:

$$C = \frac{L}{Z_0^{\,2}} = \frac{\beta}{\omega Z_0} = \frac{1}{\omega Z_0} \cdot \frac{2\pi}{\lambda}. \tag{5}$$

Using (5), we extracted the periodic shunt capacitance. Figure 3 shows the periodic capacitance of the various transmission lines on PES. For a fabrication of FTTL and FTLCGP on PES, titanium (Ti) was deposited on the PES to provide good adhesion firstly, and then gold (Au) was deposited over the Ti to reduce the resistance; the total combined thickness of the Au and Ti was 2 μm. For the FTTL, the length and width of a PMS is 160 μm and 30 μm, respectively, and the signal line width, W, is 70 μm. For the FTLCGP, the length and width of both the PMSs and the PGSs is 160 μm and 30 μm, respectively; the distance between the

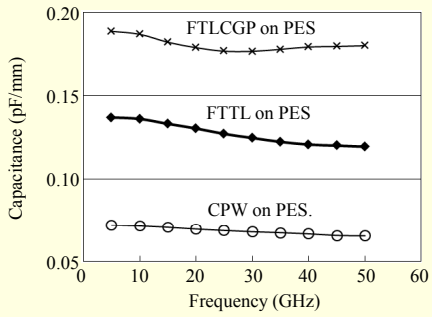

Fig. 3. Measured equivalent periodic shunt capacitance per unit length of various transmission lines on PES.

PMSs and PGSs is 30 μm; and the signal line width W is 70 μm.

As shown in this figure, FTLCGP exhibits a much higher capacitance than other structures. Concretely, the FTLCGP shows capacitance values ranging from 0.18 pF/mm to 0.19 pF/mm in the frequency range 5 GHz to 50 GHz, while the FTTL shows capacitance values ranging from 0.12 pF/mm to 0.137 pF/mm in the same frequency range. The above results reveal that using the FTLCGP structure leads to a further reduction of wavelength and characteristic impedance due to an enhancement of the periodic capacitance.

III. RF Characteristics of FTLCGP Structure on PES

Table 1 shows the wavelengths for various transmission lines on PES and silicon substrate. As shown in this table, the FTLCGP on PES exhibits shorter wavelengths than other transmission lines. In particular, compared with the FTTL on PES, the FTLCGP on PES shows a further reduction of the wavelength. The wavelength of the FTTL on PES is 2.23 mm at 50 GHz, while the wavelength of the FTLCGP on PES is 1.91 mm at the same frequency, which is 85.7% of the FTTL on PES. Compared with other transmission lines, the wavelength of the FTLCGP on PES is respectively 48.5% and 77.0% of the coplanar waveguide on PES and of the coplanar waveguide on silicon, at 50 GHz.

From Fig. 2, we can see that an increase in the length of a PMS results in an enhancement of the periodical shunt capacitance C_{PMS}, due to an increase to the open stub length, and an enhancement of coupling capacitance C_{b}, due to an increase in the coupling area between a PMS and PGS. Therefore, the characteristic impedance of the FTLCGP, Z_0, can be easily controlled by changing the length of the PMSs, because Z_0 depends on the periodic shunt capacitance and series inductance of the transmission line, as shown in (2). The dependence of Z_0 on the length of a PMS is shown in Fig. 4, where the signal line width W was fixed at 70 μm. For a

Table 1. Wavelengths of various transmission lines on PES and silicon substrate.

Frequency	FTLCGP on PES	FTTL on PES	CPW on PES	CPW on silicon
10 GHz	9.22 mm	9.79 mm	18.0 mm	10.4 mm
20 GHz	4.81 mm	5.11 mm	9.29 mm	5.71 mm
30 GHz	3.25 mm	3.56 mm	6.33 mm	3.99 mm
40 GHz	2.40 mm	2.76 mm	4.85 mm	3.04 mm
50 GHz	1.91 mm	2.23 mm	3.94 mm	2.48 mm

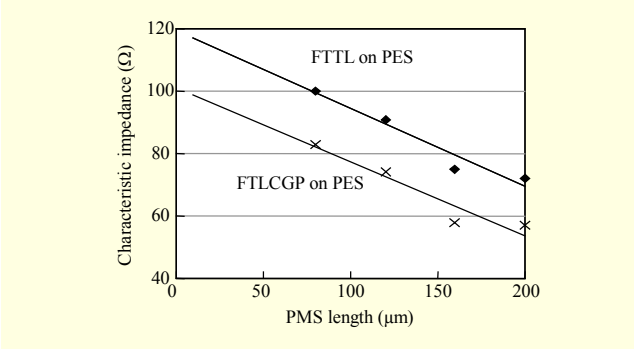

Fig. 4. Characteristic impedance of FTLCGP structure on PES.

comparison, we also plotted the Z_0 of the FTTL. As shown in this figure, an FTLCGP with various characteristic impedance can be realized on PES substrate by changing only the length of the PMSs. From the above result, we must pay attention to one important result. As mentioned before, the transmission line on the PES showed a much higher characteristic impedance than that on a conventional semiconducting substrate. Therefore, a transmission line with a very wide line width is required for low impedance matching applications [4]. The FTTL on PES showed a characteristic impedance that was lower than that of a conventional coplanar waveguide on PES [4]. According to the above result, however, the FTLCGP shows a further reduction of characteristic impedance compared with the FTTL, which originates from an increase in the periodic shunt capacitance. In other words, compared with the FTTL, the periodic shunt capacitance of the FTLCGP was enhanced due to the coupling between PMSs and PGSs, and from (2), we can see that an increase to the periodic shunt capacitance reduces the characteristic impedance. Therefore, if a transmission line with the same characteristic is fabricated on PES, then the line width of FTLCGP is much narrower than the FTTL. Concretely, the PMS length of the FTLCGP with a Z_0 of 61 Ω is 0.15 mm, and the total line width is 0.37 mm, while the PMS length of the FTTL with the same Z_0 is 0.23 mm, and the total line width is 0.53 mm. The above results indicate that using the FTLCGP can lead to a further reduction of device size on PES.

Table 2. Insertion loss of FTLCGP and coplanar waveguide on PES with a length of λ/4.

Frequency	FTLCGP on PES	CPW on PES
10 GHz	1.59 dB	1.34 dB
20 GHz	1.75 dB	1.55 dB
30 GHz	1.13 dB	1.69 dB
40 GHz	1.00 dB	1.53 dB

Until now, various types of periodic structures have been studied for application to RF circuits [7]–[13]. In particular, a slow-wave structure with an FTLCGP was fabricated on a PCB for use with a low-impedance transmission line in S-band [7]. The slow-wave structure successfully operated as a transmission line up to S-band. However, slow-wave structures on conventional PCBs, such as Teflon, show very narrow band characteristics and very high losses in high-frequency ranges. However, the FTLCGP fabricated on PES showed a very low loss up to the millimeter wave range. Table 2 shows the insection loss of the FTLCGP and coplanar waveguide on PES. For a fair loss comparison, two transmission lines of the same electrical length should be compared, because the wavelengths of the two transmission lines are different from each other. Therefore, the loss of two transmission lines of length λ/4 were compared. As shown in this table, the FTLCGP on PES shows a low loss, which is comparable to the coplanar waveguide on PES. Concretely, the FTLCGP on PES shows a loss of 1 dB to 1.75 dB in the range 10 GHz to 40 GHz, and the coplanar waveguide on PES shows a loss of 1.34 dB to 1.69 dB in the same frequency range. This low loss of the transmission lines on PES originates from the good electrical insulating properties of PES [4]. The above results indicate that the FTLCGP can be employed for application in flexible passive devices up to the millimeter wave frequency due to its low loss characteristic. Incidentally, the insertion loss of the FTLCGP decreases from 20 GHz to 40 GHz. This result is caused by the characteristic of the attenuation constant, α. It is known that the attenuation constant α of a transmission line on semiconducting substrate saturates in a certain frequency range [13], which causes a decrease in the rate of insertion loss per wavelength.

Figure 5 shows the measured propagation constant (β) of the FTLCGP and of the other types of transmission lines on PES and silicon substrate. According to our previous results [4], the FTTL on PES exhibited a higher β than that exhibited by other types of transmission lines due to its strong slow-wave

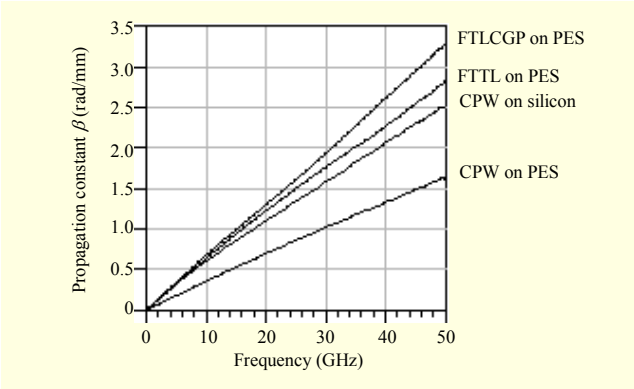

Fig. 5. Measured propagation constant β of various transmission lines on PES and silicon substrate.

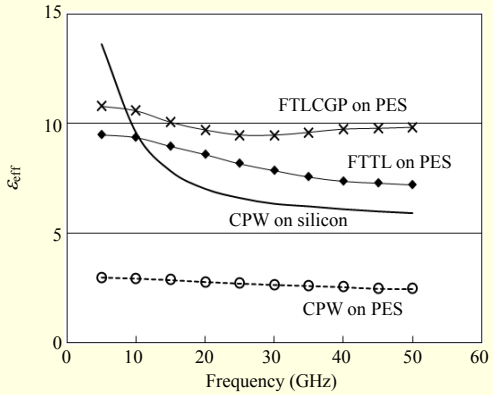

Fig. 6. Effective permittivity ε_{eff} of various transmission lines on PES and silicon substrate.

characteristic [4]. As shown in Fig. 5, however, the FTLCGP exhibits a higher β than that exhibited by the FTTL. Concretely, the FTLCGP on PES shows values of β ranging from 0.68 rad/mm to 3.28 rad/mm in the range 10 GHz to 50 GHz, while the FTTL on PES shows values of β ranging from 0.64 rad/mm to 2.8 rad/mm in the same frequency range. The above result is due to the high periodic capacitance value of the FTLCGP. According to transmission line theory, β is proportional to the square root of the periodic capacitance, which can be expressed in the following equations [6]:

$$\beta = \omega\sqrt{\mu\varepsilon} = \omega\sqrt{\mu\varepsilon_0\varepsilon_{eff}} = \omega\sqrt{LC}, \quad (6)$$

where ε_0, μ, and ε_{eff} represent the permittivity of air, permeability, and effective permittivity of the transmission line, respectively. From (6), we can see that the higher the value of the periodic capacitance, the higher the value of β. As shown in Fig. 3, the FTLCGP showed a higher periodic capacitance value than that of the FTTL, which led to a higher value of β. The larger the value of β for the FTLCGP, the shorter the wavelength, as shown in Table 1.

We also investigated the effective permittivity ε_{eff} of the FTLCGP on PES. The ε_{eff} was obtained from the following equation:

$$\varepsilon_{eff} = \left(\frac{2\pi}{\omega\lambda}\cdot\frac{1}{\sqrt{\varepsilon_0\mu_0}}\right)^2, \quad (7)$$

where λ and μ_0 represent the wavelength of the transmission line and permeability of air, respectively. Figure 6 shows the effective permittivity ε_{eff} of the FTLCGP and other types of transmission lines. As shown in Fig. 6, the FTLCGP displays a higher effective permittivity than that displayed by the FTTL and coplanar waveguide on PES, due to its strong slow-wave characteristic. Concretely, the FTLCGP displays an ε_{eff} of 9.46 to 10.6 in the range 5 GHz to 50 GHz, while the FTTL displays an ε_{eff} of 7.2 to 9.5 in the same frequency range. In particular, the FTLCGP on PES exhibits a higher ε_{eff} than that exhibited by the coplanar waveguide on silicon substrate in a frequency range higher than 10 GHz. Therefore, for the fabrication of passive components, using the FTLCGP enables a further reduction of component size compared with other types of transmission lines, because the higher the ε_{eff} of the semiconducting substrate, the smaller the component size on the semiconducting substrate [6]. From Fig. 6, we can see that the coplanar waveguide on silicon substrate exhibits a strong frequency dispersion characteristic. Generally, a slow-wave mode of propagation, as well as a quasi-transverse electromagnetic (quasi-TEM) mode, exists on oxide/silicon substrate, which leads to a strong frequency dispersion characteristic [13]. On the other hand, the transmission line on PES exhibits a very weak frequency dispersion characteristic due to its dominant quasi-TEM mode on the metal/high-insulating substrate structure [14]. Notably, in spite of its composite periodic structure, the FTLCGP exhibits a frequency dependency that is weaker than that exhibited by the FTTL and has good frequency dispersion characteristics comparable to the coplanar waveguide on PES. This can be explained as follows. As mentioned before, there is a coupling capacitance between the PMSs of the FTTL structure. However, this coupling capacitance is only a parasitic capacitance, and as such, it cannot contribute to a reduction of wavelength. Therefore, this parasitic capacitance causes a relatively strong frequency dispersion characteristic. However, there is a coupling shunt capacitance between the signal line and ground in the FTLCGP, which is a part of the equivalent shunt capacitance of the transmission line, not a parasitic capacitance. This shunt capacitance doesn't cause a strong frequency dispersion, and it only contributes to a reduction of wavelength [6]. The above results reveal that the FTLCGP structure on PES can be effectively used for broadband applications due to its very weak frequency dispersion characteristic. Using the effective permittivity equation model

of the coplanar waveguide, we also extracted the relative permittivity of the PES from the effective permittivity shown in Fig. 6. According to the result, the relative permittivity of the PES was 3.4 to 3.6 in the above frequency range.

IV. Theoretical Analysis of FTLCGP Structure on PES

In this work, the RF characteristics of the FTLCGP on PES were theoretically studied using a simple equivalent circuit [6] and closed-form equations. Concretely, RF characteristics, such as impedance and bandwidth, were extracted from the simple theoretical analysis. The FTLCGP structure can be expressed as the periodically loaded line shown in Figs. 7(a) and 7(b), and C_{FTLCGP} is the periodical capacitance of the FTLCGP structure, which is shown in Fig. 3. In this figure, d is the length of a unit cell in the periodic structure, which for the FTLCGP, is equal to 120 μm. The periodically loaded line shown in Fig. 7(a) can also be expressed by the periodical susceptance, jb, shown in Fig. 7(b). The periodical susceptance jb is given by

$$jb = j\omega C_{FTLCGP} / Y_0 = j\omega C_{FTLCGP} Z_0, \tag{8a}$$

$$b = \omega C_{FTLCGP} Z_0, \tag{8b}$$

where ω and Z_0 are the angular frequency and characteristic impedance of the transmission line without periodic structure, respectively.

For a theoretical analysis of the transmission line employing FTLCGP, we begin by studying the propagation characteristics of the equivalent circuit shown in Fig. 7(b). Each unit cell of this line is of length d, with a shunt susceptance across the midpoint of this length, and the susceptance jb is normalized to the characteristic impedance, as shown in (8b). From Fig. 7(b), we can relate the voltages and currents on either side of the nth unit cell using the following ABCD matrix:

$$\begin{bmatrix} V_n \\ I_n \end{bmatrix} = \begin{bmatrix} A & B \\ C & D \end{bmatrix} \begin{bmatrix} V_{n+1} \\ I_{n+1} \end{bmatrix}, \tag{9}$$

where A, B, C, and D are the matrix parameters for the unit cell shown in Fig. 7. The unit cell consists of two lines of length $d/2$ and susceptance b. In addition, in (9), I_n and V_n are the current and voltage at the input of nth unit cell shown in Fig. 7, respectively, and I_{n+1} and V_{n+1} are the current and voltage at the output of the $(n+1)$th unit cell, respectively.

The matrix parameters can be given by [6]

$$\begin{bmatrix} A & B \\ C & D \end{bmatrix} = \begin{bmatrix} \cos\frac{kd}{2} & j\sin\frac{kd}{2} \\ j\sin\frac{kd}{2} & \cos\frac{kd}{2} \end{bmatrix} \begin{bmatrix} 1 & 0 \\ jb & 1 \end{bmatrix} \begin{bmatrix} \cos\frac{kd}{2} & j\sin\frac{kd}{2} \\ j\sin\frac{kd}{2} & \cos\frac{kd}{2} \end{bmatrix}$$
$$= \begin{bmatrix} (\cos kd - \frac{b}{2}\sin kd) & j(\sin kd + \frac{b}{2}\cos kd - \frac{b}{2}) \\ j(\sin kd + \frac{b}{2}\cos kd + \frac{b}{2}) & (\cos kd - \frac{b}{2}\sin kd) \end{bmatrix}, \tag{10a}$$

$$kd = \omega\sqrt{LC_a}\,d = \omega\sqrt{\mu_0\varepsilon_0\varepsilon_{eff}}\,d, \tag{10b}$$

where μ_0 and ε_0 are the permeability and permittivity of air, respectively. The effective permittivity ε_{eff} is shown in Fig. 6. In Fig. 7, the transmission line with a length of $d/2$ can be expressed by an LC equivalent circuit, and the C_a was considered when the propagation constant (k) of the line itself was calculated using (10a) and (10b). Using the propagation constant γ of the guided wave on the periodically loaded microstrip line gives

$$V_{n+1} = V_n e^{-\gamma d}, \tag{11a}$$

$$I_{n+1} = I_n e^{-\gamma d}. \tag{11b}$$

Using (9), (11a), and (11b) gives [6]

$$\begin{bmatrix} V_n \\ I_n \end{bmatrix} = \begin{bmatrix} A & B \\ C & D \end{bmatrix} \begin{bmatrix} V_{n+1} \\ I_{n+1} \end{bmatrix} = \begin{bmatrix} V_{n+1}e^{\gamma d} \\ I_{n+1}e^{\gamma d} \end{bmatrix},$$
$$\begin{bmatrix} A - e^{\gamma d} & B \\ C & D - e^{\gamma d} \end{bmatrix} \begin{bmatrix} V_{n+1} \\ I_{n+1} \end{bmatrix} = \begin{bmatrix} 0 \\ 0 \end{bmatrix}. \tag{12}$$

For a nontrivial solution,

$$AD + e^{2\gamma d} - (A+D)e^{\gamma d} - BC = 0.$$

Since $AD - BC = 1$ for a lossless network, the above equation can be expressed as

$$1 + e^{2\gamma d} - (A+D)e^{\gamma d} = e^{-\gamma d} + e^{\gamma d} - (A+D) = 0. \tag{13}$$

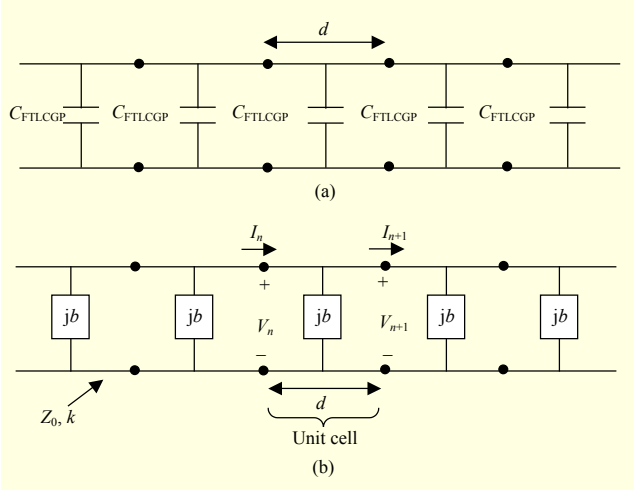

Fig. 7. Equivalent circuit of FTLCGP structure on PES: (a) an equivalent circuit with periodically loaded capacitor C_b and (b) an equivalent circuit with periodically loaded susceptance jb.

Using (10) and (3) gives

$$\frac{e^{-\gamma d}+e^{\gamma d}}{2}=\cosh\gamma d=\frac{(A+D)}{2}=(\cos kd-\frac{b}{2}\sin kd), \quad (14)$$

where (10) was used for the values of A and D. Since the propagation constant γ of the guided wave on the periodically loaded microstrip line consists of real and imaginary parts, it can be represented by

$$\gamma=\alpha+\mathrm{j}\beta. \quad (15)$$

Thus, from (14) and (15), the following expression can be obtained:

$$\cosh\gamma d=\cosh\alpha d\cos\beta d+\mathrm{j}\sinh\alpha d\sin\beta d=\cos kd-\frac{b}{2}\sin kd. \quad (16)$$

Since the right-hand side of (16) is real, we should have either $\sinh \alpha d = 0$ or $\sin \beta d = 0$. If the attenuation constant α is 0, then this corresponds to the case of a non-attenuating propagation wave on the periodic structure and defines the passband of the structure. Then, (16) can be expressed as follows:

$$\cosh \mathrm{j}\beta d=\cos\beta d=\cos kd-\frac{b}{2}\sin kd=\cos kd-Xkd\sin kd, \quad (17a)$$

where

$$X=\left(\frac{C_{\mathrm{FTLCGP}}Z_0}{2\sqrt{\varepsilon_{\mathrm{eff}}}\sqrt{\mu_0\varepsilon_0}d}\right). \quad (17b)$$

Note that there are an infinite number of values of β that can satisfy (17). If the attenuation constant α is not zero, then the wave is attenuated along the line, and this case corresponds to that of a stopband. In this case, (16) reduces to

$$\cosh\alpha d=\left|\cos kd-Xkd\sin kd\right|\geq 1. \quad (18)$$

Thus, depending on the frequency and normalized susceptance values, the periodically loaded line will exhibit either passbands or stopbands, and as such, it can be considered as a type of filter. Figure 8 shows the passbands and stopbands calculated from (17) and (18). Using (8), (17), and (18), we can obtain the bandwidth of the pass- and stopbands from the βd - kd graph of Fig. 8. The bandwidths of the FTLCGP structure are summarized in Table 3. In this table, the first passband corresponds to a practical bandwidth. From the table, we can see that the FTLCGP structure has a cut-off frequency of 280 GHz, which means that it can be used as a transmission line in millimeter wave and microwave frequencies.

From (17), we can obtain the following equations:

$$\beta=\frac{\cos^{-1}(\cos kd-Xkd\sin kd)}{d}, \quad (19)$$

$$\lambda=\frac{2\pi}{\beta}=\frac{2\pi d}{\cos^{-1}(\cos kd-Xkd\sin kd)}. \quad (20)$$

Table 3. Bandwidths of FTLCGP structure on PES.

	Frequency range (GHz)	Bandwidth (GHZ)
First passband	≤ 280	280
First stopband	281–759	479
Second passband	760–860	101
Second stopband	861–1,518	658

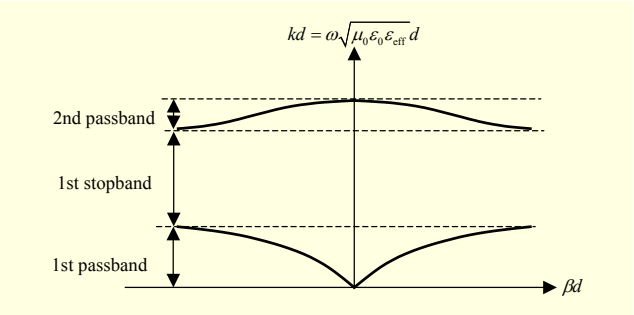

Fig. 8. Passbands and stopbands calculated from βd-kd relations of (17) and (18).

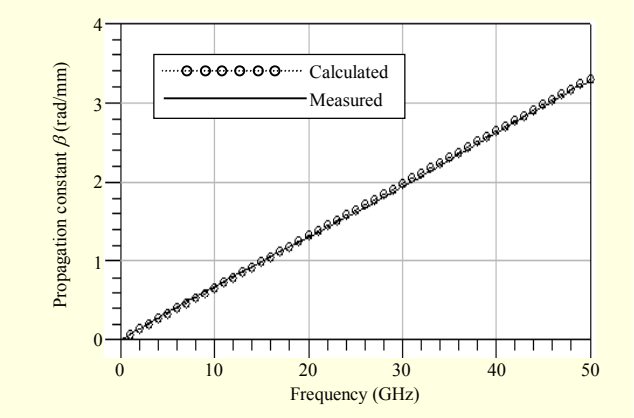

Fig. 9. Measured and calculated propagation constant of FTLCGP on PES.

From the above equations, we can calculate the propagation constant and wavelength. Figures 9 and 10 show the propagation constant and wavelength calculated from the above equations, which were compared with measured results. Form this, we can see that the calculated results show good agreement with the measured ones, which indicates that the above theoretical method is fairly accurate.

Besides the propagation constant of the waves on the periodically loaded line, we are also interested in the characteristic impedance for these waves. We can define the characteristic impedance at the unit cell terminal as

$$Z_{\mathrm{B}}=Z_0\frac{V_{n+1}}{I_{n+1}}, \quad (21)$$

ETRI Journal, Volume 37, Number 1, February 2015
http://dx.doi.org/10.4218/etrij.15.0114.0244

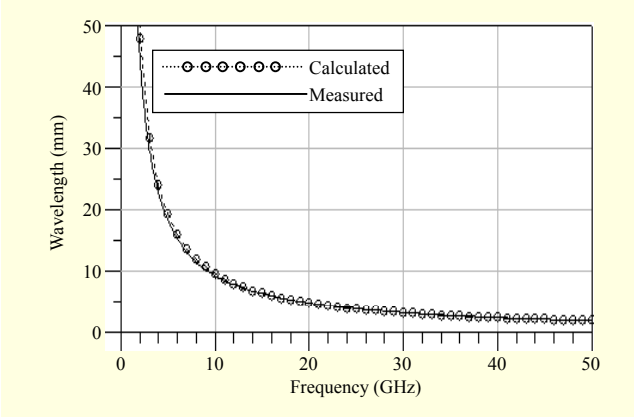

Fig. 10. Measured and calculated wavelength of FTLCGP on PES.

since V_{n+1} and I_{n+1} in the above derivation are normalized quantities. Equation (12) can be expressed as

$$(A - e^{\gamma d})V_{n+1} + BI_{n+1} = 0. \tag{22}$$

If the ratio of voltage to current obtained from (22) is substituted into (21), then we can obtain following equation:

$$Z_B = \frac{-BZ_0}{(A - e^{\gamma d})}. \tag{23}$$

From (13), we can solve for $e^{\gamma d}$ in terms of A and D to achieve the following:

$$e^{\gamma d} = \frac{(A+D) \pm \sqrt{(A+D)^2 - 4}}{2}. \tag{24}$$

Because A is equal to D ($A = D$), using (10), (23), and (24) gives

$$Z_B = \frac{\left|(\sin kd + \frac{b}{2}\cos kd - \frac{b}{2})\right| \cdot Z_0}{\sqrt{1 - (\cos kd - \frac{b}{2}\sin kd)^2}}. \tag{25}$$

The characteristic impedance, Z_B, can be calculated from (8) and (25). Figures 11(a) and 11(b) show the calculated characteristic impedance and measured return loss for the FTLCGP on PES. In Fig. 11(b), the return loss was measured with a port impedance of 58 Ω from 0.1 GHz to 50 GHz, and the return loss values ware less than –25 dB in this frequency range, which means that the measured characteristic impedance is 58 Ω. From this result, we can see that the calculated result shows good agreement with the measured one.

We also calculated the effective permittivity ε_{eff} of the FTLCGP on PES. Using (7) and (20) leads to the following equation:

$$\varepsilon_{eff} = \left(\frac{\cos^{-1}(\cos kd - Xkd \sin kd)}{\omega d \sqrt{\varepsilon_0 \mu_0}} \right)^2. \tag{26}$$

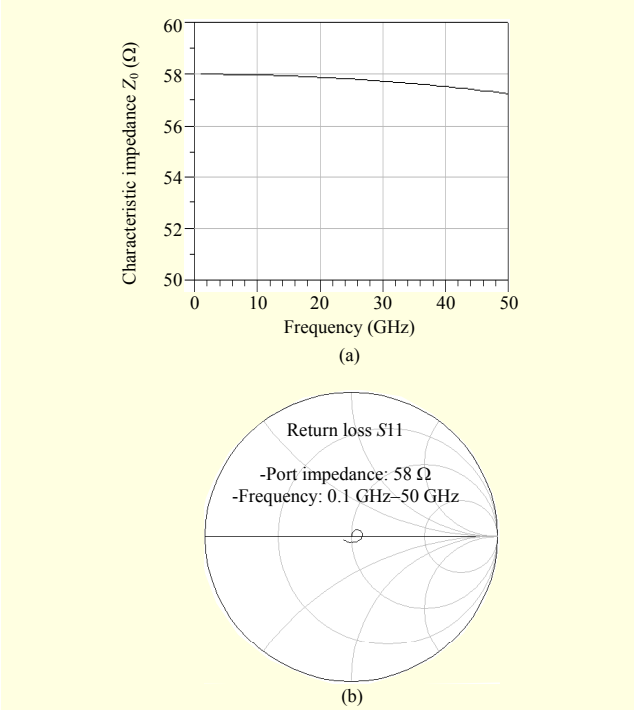

Fig. 11. RF characteristic of FTLCGP structure on PES: (a) calculated characteristic impedance and (b) measured return loss at a port impedance of 58 Ω.

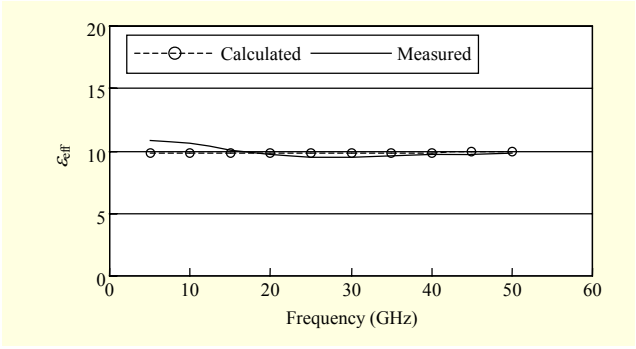

Fig. 12. Measured and calculated effective permittivity ε_{eff} of FTLCGP on PES.

Using (26), we calculated the effective permittivity. Figure 12 shows the measured and calculated effective permittivity of the FTLCGP on PES. As shown in this figure, the calculated result shows good agreement with the measured one.

V. Conclusion

In this work, we investigated the RF characteristics of the FTLCGP structure on PES substrate. The FTLCGP on PES exhibited much higher periodic shunt capacitance values than

those exhibited by other types of transmission lines due to the coupling capacitance between the PMSs and PGSs, which resulted in a further reduction of wavelength. For example, the wavelength of the FTLCGP on PES was 1.91 mm at 50 GHz, which was 85.7% of the FTTL on PES and 48.5% of the coplanar waveguide on PES. The characteristic impedance Z_0 of the FTLCGP structure could be easily controlled by changing only the length of the PMSs. The FTLCGP showed a lower characteristic impedance than that shown by the FTTL due to its higher periodic shunt capacitance, which resulted in a reduction of line width. Concretely, the total line width of the FTLCGP with a Z_0 of 61 Ω was 0.37 mm, while the total line width of the FTTL with the same Z_0 was 0.53 mm. According to the results, we can see that, compared with the FTTL, the FTLCGP is more suitable for RF applications due to its shorter wavelength and narrower line width. The FTLCGP on PES exhibited a low loss of 1 dB to 1.75 dB in the range 10 GHz to 40 GHz, which was comparable to the conventional coplanar waveguide on PES. In addition, the FTLCGP structure exhibited a much higher propagation constant β and effective permittivity ε_{eff} than that exhibited by other types of transmission lines on PES due to its strong slow-wave characteristic. Notably, in spite of its composite periodic structure, the FTLCGP showed a weaker frequency dependency than that shown by the FTTL, as well as a good frequency dispersion characteristic comparable to the conventional coplanar waveguide on PES. The FTLCGP structure showed an ε_{eff} of 9.46 to 10.6 in the range 5 GHz to 50 GHz. The above results reveal that the FTLCGP on PES can be effectively used with a broadband and low loss characteristic in RF components.

The RF characteristics of the FTLCGP on PES were studied using a simple equivalent circuit and closed-form equations. RF characteristics, such as impedance and bandwidth, were extracted from the simple theoretical analysis, which offered a design guideline for passive components employing FTLCGP. According to the results, it was found that the theoretical results showed good agreement with the experimental ones. Using the theoretical analysis, we also extracted the bandwidth characteristic of the FTLCGP on PES. The FTLCGP structure showed a cut-off frequency of 280 GHz, which means that it can be used as a transmission line up to the millimeter wave frequency range. From these results, we can see that the FTLCGP structure on PES is a promising candidate for use with RF transmission lines on flexible substrates.

References

[1] Y. Sun and J.A. Rogers, "Inorganic Semiconductors for Flexible Electronics," *Adv. Mater*., vol. 19, no. 15, Aug. 2007, pp. 1897–1916.

[2] E. Celik et al., "Carbon Nanotube Blended Polyethersulfone Membranes for Fouling Control in Water Treatment," *Water Res*., vol. 45, no. 1, Jan. 2011, pp. 274–282.

[3] R. Rajasekaran, M. Alagar, and C.K. Chozhan, "Effect of Polyethersulfone and N, N'-Bismaleimido-4, 4'-Diphenyl Methane on the Mechanical and Thermal Properties of Epoxy Systems," *Exp. Polymer Lett*., vol. 2, no. 5, 2008, pp. 339–348.

[4] Y. Yun, H.S. Kim, and N. Jang, "Study on Characteristics of Various RF Transmission Line Structures on PES Substrate for Application to Flexible MMIC," *ETRI J*., vol. 36, no. 1, Feb. 2014, pp. 106–115.

[5] Y. Yun et al., "A Miniaturized Impedance Transformer on PES for Flexible RFICs," *Microw. J*., vol. 57, no. 2, Feb. 2014, pp. 100–110.

[6] D.M. Pozar, "*Microw*ave *Engineering*," Reading, MA, USA: Addison-Wesley, 1990.

[7] T. Fujii et al., "Miniature Broad-Band CPW 3 dB Branch-Line Couplers in Slow-Wave Structure," *IEICE Trans. Electron*., vol. E90-C, no. 12, Dec. 2007, pp. 2245–2253.

[8] D. Ahn et al., "A Design of Low-Pass Filter Using the Novel Microstrip Defected Ground Structure," *IEEE Trans. Microw. Theory Techn*., vol. 49, no. 1, Jan. 2001, pp. 86–93.

[9] F.-R. Yang et al., "A UC-PBG Structure and Its Applications for Microwave Circuits," *IEEE Trans. Microw. Theory Techn*., vol. 47, no. 8, Aug. 1999, pp. 1509–1514.

[10] A.S. Andrenko, Y. Ikeda, and O. Ishida, "Application of PBG Microstrip Circuits for Enhancing the Performance of High-Density Substrate Patch Antennas," *Microw. Opt. Techn. Lett.*, vol. 32, no. 5, Mar. 2002, pp. 340–344.

[11] A. Lai and T. Itoh, "Microwave Composite Right/Left-Handed Metamaterials and Devices," *Asia-Pacific Microw. Conf*., Suzhou, China, Dec. 4–7, 2005, pp. 31–34.

[12] J. Gao and L. Zhu, "Per-Unit-Length Parameters of 1-D CPW Metamaterials with Simultaneously Series-C and Shunt-L Loading," *Asia-Pacific Microw. Conf*., Suzhou, China, Dec. 4–7, 2005, pp. 39–42.

[13] J.R. Long, "Passive Components for Silicon RF and MMIC Design," *IEICE Trans. Electron*., vol. E86-C, no. 6, June 2003, pp. 1022–1031.

[14] J. Zhang and T.Y. Hsiang, "Dispersion Characteristics of Coplanar Waveguides at Subterahertz Frequencies," *Progress Electromag. Res. Symp*., Cambridge, MA, USA, vol. 2, no. 3, Mar. 2006, pp. 232–235.

Young Yun received his BS degree in electronic engineering from Yonsei University, Seoul, Rep. of Korea in 1993; his MS in electrical and electronic engineering from Pohang University of Science and Technology, Pohang, Rep. of Korea in 1995; and his PhD in electrical engineering from Osaka University, Osaka, Japan, in 1999. From 1999 to 2003, he worked as an engineer for the Matsushita Electric Industrial Company Ltd. (Panasonic), Osaka, Japan, where he was engaged in the research and development of monolithic microwave ICs (MMICs) for wireless communications. In 2003, he joined the Department of Radio Communication Engineering, Korea Maritime and Ocean University, Busan, Rep. of Korea. He is currently a professor, and his research interests include design and measurement for RF/microwave and millimeter-wave IC and design and fabrication for HEMT and HBT. Since 2008, he has served as an associate editor of the Institute of Electronics, Information and Communication Engineers (IEICE) in Japan and as an editor of the Korean Society of Marine Engineering in the Rep. of Korea. He is the author and co-author of over 110 internationally published journal papers and 15 patents pending in RF/microwave devices and ICs.

Jang-Hyeon Jeong received his BS and MS degrees in radio communication engineering from the Korea Maritime and Ocean University, Busan, Rep. of Korea, in 2010 and 2012, respectively, and is currently working toward his PhD in radio communication engineering.

Hong Seung Kim received his BS, MS, and PhD degrees in materials science and engineering from the Korea Advanced Institute of Science and Technology, Daejeon, Rep. of Korea, in 1990, 1993, and 1999, respectively. He joined the Electronics and Telecommunications Research Institute, Daejeon, Rep. of Korea, in 1999 and has worked on the fabrication and development of SiGe heterojunction bipolar transistors (HBTs) and InP/InGaAs HBTs for OEIC. From 2001 to 2002, he was a post-doctoral research associate in electrical engineering at Cornell University, Ithaca, NY, USA, where he worked on three-dimensional integration. In 2003, he joined the Depaprtment of Nano Semiconductor Engineering, Korea Maritime and Ocean University, Busan, Rep. of Korea. He is currently a professor, and his research interests include optoelectronic properties of ZnO-based devices, such as UV LEDs and transparent transistors.

Nakwon Jang received his BS, MS, and PhD degrees in electrical engineering from Yonsei University, Seoul, Rep. of Korea, in 1990, 1992, and 1999, respectively. From 1992 to 1995, he was with Samsung Electronics, Yongin, Rep. of Korea, where he was involved in the design of video-signal driver circuits for p-Si TFT LCDs. After completing his PhD, he worked as a senior engineer in the Semiconductor R&D Division of Samsung Electronics, where he was engaged in the research and development of 4 MB and 32 MB FRAM. He joined the Korea Maritime and Ocean University as a professor in the Department of Electrical and Electronics Engineering in Busan, Rep. of Korea, in September 2003. He is currently a professor, and his research interests include the design and fabrication of LEDs and ZnO TFTs. He is the author and co-author of over 70 journal articles on semiconductor devices.